Journal of Marine Research, 52, 559–581, 1994

Journal of
MARINE RESEARCH

Volume 52, Number 4

Vortex pair model of Langmuir circulation

by G. T. Csanady[1]

ABSTRACT

Accumulating evidence shows spacing and length of surface convergences associated with Langmuir circulation to be random variables, their strength also variable, their lifetime limited. Analysis of several sets of quantitative observations reveals the probability distribution of windrow spacing to be lognormal. This suggests generation of surface convergences at random times and locations on the sea surface.

Moving shear stress anomalies, under wind gusts or breaking long waves, are capable of generating surface convergence in their wakes, and are the type of random event likely responsible for the stochastic properties of windrows. The generation mechanism envisaged is a "forced" version of the Craik-Leibovich "CL2" theory, Stokes drift tilting the vertical vortex lines at the edges of stress anomalies. This contrasts with the feedback mechanism of the CL2 theory operating on infinitesimal spanwise disturbances. Realistic shear stress anomalies produce vortex pairs strong enough to account for Langmuir circulation without feedback amplification.

A vortex pair just under the sea surface induces motion bringing the vortices together at first, and then causing them to dive deep into the mixed layer. This inviscid kinematic effect limits the surface presence of convergences, and accounts for the finite lifetime of windrows without even taking into account viscous decay.

Converging motion at the surface, and low eddy viscosity, combine to channel the downward momentum transfer from the air flow into descending branches of the Langmuir circulation. One result is the increase of windward surface velocity in the convergences.

1. Introduction

"Langmuir circulation" is a conceptual model of the flow field responsible for long lines of surface convergence on a wind-blown water surface, collecting floating

1. Center for Coastal Physical Oceanography, Old Dominion University, Norfolk, Virginia, 23529, U.S.A.

particles into windrows. Langmuir (1938) first carried out systematic field observations on windrows, and postulated adjacent streamwise (parallel to the wind) vortices, of opposite sense of rotation, to maintain the convergences, coexisting with the wind-driven shear flow. His observations also established that wind generates the vortices, not convective instability, that the downwelling motion under the convergences is more intense than the compensating upwelling, and that the downwind motion of the water in the convergences is faster than outside.

Later work added much to the empirical picture. Earlier reviews of the evidence tended to stress the features already recognized by Langmuir (Scott *et al.,* 1969; Faller, 1971; Leibovich, 1983), others pointing out discrepancies (Pollard, 1977; Gargett, 1989; Thorpe, 1992), often revealed by novel or more sophisticated methods of observation. Variability of the windrow structure is the general theme of this recent evolution of Langmuir's ideas: observations show statistical distributions of the spacing or length of windrows, indicate varying strength and finite lifetime of the convergences. This aspect of the evidence is discussed in detail below.

Several authors have proposed theories to explain the generation of Langmuir circulation. As Leibovich (1983) makes clear, all of the early theories fail on empirical or theoretical grounds, except the later version of the wave-current interaction theory due to Craik and Leibovich (1976). This theory, labeled CL2, was introduced by Craik (1977), and developed further by Leibovich and his collaborators, Leibovich and Paolucci (1980), Cox and Leibovich (1993), Leibovich and Tandon (1993), see also other papers referenced by them. The theory rests on the recognition that a combination of two-dimensional shear flow (in the xz plane, driven by the wind), with irrotational Stokes drift of the wind-wave field, is unstable to spanwise (y) disturbances. The basic premise of the theory is that infinitesimal spanwise sinusoidal disturbances grow into the streamwise vortices of Langmuir circulation. As in all such instability theories, a key result is the wavenumber of the disturbance with the highest growth rate, but the eigenfunctions also suggest the form of the disturbance and finite amplitude calculation reveals details of the evolution of vortices (see e.g. Leibovich and Paolucci, 1980).

The CL2 theory is certainly sound, and it yields the important physical insight of Stokes drift-vortex interaction. As the theory stands, however, it does not clearly explain Langmuir circulation. The usual verification of an instability theory consists of observing disturbances of the highest growth rate to appear first, or to dominate. This has not been forthcoming. One may still argue that initial Langmuir circulation (as the wind begins to blow) is according to the theory, but difficult to observe, while later it becomes more chaotic, in analogy with Tollmien-Schlichting waves and turbulence. If this were so, Langmuir circulation would still be maintained by Stokes drift-basic shear flow interaction.

An alternative possibility is that strong external forcing replaces the feeble mechanism of CL2 instability, at least to start Langmuir circulation. If instead of an

infinitesimal disturbance, Stokes drift were to act on more substantial vertical vorticity, generated by an external force, generation of Langmuir circulation would be much more robust. Furthermore, externally generated vertical vorticity could conceivably interact with the shear flow, as well as with Stokes drift, to generate streamwise vorticity.

Wind gusts and breaking long waves locally increase surface shear and generate vertical vorticity at their edges. An analysis of their flow field shows that the resulting vertical vorticity-Stokes drift interaction is indeed strong enough to establish Langmuir circulation (but vortex interaction without Stokes drift is not). The random occurrence of such "moving shear stress anomalies" helps explain the variability of windrow spacing and strength. The model of streamwise vorticity generation associated with wind gusts or breaking waves may be thought of as the "forced" version of the CL2 theory, relying on impressed, instead of spontaneously arising, occurrence of vertical vorticity.

Another kind of hydrodynamic instability, possibly accounting for windrow length variability, affects an array of parallel streamwise vortices. This has recently been examined by Thorpe (1992). The kinematics of a vortex pair, left behind by a passing shear stress anomaly, is a further source of variability: inviscid vortex interaction causes such vortices to approach each other, then to dive down deep into the mixed layer. Such vortex behavior may well account for the life cycle of a windrow: the convergence intensifies as the vortices approach, then decays as they drive. This idea is also discussed below in greater detail.

2. Windrow variability

In a remarkably thorough study, conducted with the simplest methods of observation, Langmuir (1938) discovered the now well known flow field of windrows: adjacent counterrotating vortices generating surface convergences; floating objects collecting where the water sinks; individual water particles moving in helical paths, faster in the convergences than outside. Langmuir found the sinking motion in the convergences to be fairly slow, of order 3 cm s^{-1}, the compensating upward motion outside the vortices much slower still. Windrows are present in moderate to strong winds, whether the surface heat flux is upward or downward, so that they cannot be attributed to thermal convection.

Many later field studies of Langmuir circulation confirmed and fleshed out these findings, see review articles of Scott *et al.* (1969), Faller (1971), Pollard (1977), Leibovich (1983), and Gargett (1989). More recently, sophisticated new methods of observation revealed further details (Thorpe and Hall, 1982; Weller *et al.,* 1985; Smith *et al.,* 1987; Weller and Price, 1988; Zedel and Farmer, 1991). As far as the flow field of the Langmuir vortices is concerned, the only major departure has been Weller *et al.*'s and Weller and Price's finding of vertical motion an order of magnitude faster than Langmuir's results showed, (up to 30 cm s^{-1}), in the middle of

the mixed layer (at 20 m depth), rather than only near the surface, as most other observations show. The windward current anomaly at the same location was similarly large, implying downward momentum advection at a rate locally hundreds of times greater than the wind stress. Such vigorous vertical motions must be confined to a small fraction of the water surface.

Past reviews of Langmuir circulation have not stressed quantitative aspects of windrow variability. The occurrence of windrows under wind of given strength (always with enough floating objects present to mark them: a trivial point is that one does not see a windrow unless some floating material marks it) is only statistically predictable: Welander (1963), for example, reported that they are always absent in winds weaker than 4 m s^{-1}, always present above 7 m s^{-1}, except in rain, with a gradual increase of their probability in between. Furthermore, the question, do we see windrows?, is sometimes difficult to answer. In a summer-long series of 246 observations on Lake Huron, using confetti and aluminium powder to mark surface convergences, we found 77 "doubtful" cases in weak winds (Csanady, 1965), suggesting perhaps an incompletely developed tendency to windrow generation. We also noted a statistically clear relationship to wind speed, similar to Welander's conclusions, as did Scott *et al.* (1969), see the latter authors' histogram of windrow probability, reproduced here in Figure 1.

The question of windrow spacing has attracted much attention in the literature. Most observers reported a single or "dominant" spacing, of the order of mixed layer depth, sometimes qualified with remarks about shorter or less well developed windrows between major ones, or some other hint at a random distribution of spacing. A few authors were, fortunately, more quantitative and reported histograms of spacing (Faller and Woodcock, 1964; Kenney, 1977; Thorpe and Hall, 1982; Zedel and Farmer, 1991). The sample size (number of windrows crossed by a boat steaming crosswind, or counted in an areal photograph) was usually insufficient to define a smooth distribution, except in Kenney's observations (several hundred). Kenney showed that all his spacing distributions (19 of them) approximated a log-normal model as well as could be expected for the sample sizes. Figure 2 shows one of Kenney's histograms and a log-normal curve fitted by him. Figures 3 and 4 show cumulative frequency versus spacing on log-probability paper, 3a and 4a, and also frequency histogram versus spacing, 3b and 4b, of one set of observations each by Thorpe and Hall (1982) and Zedel and Farmer (1991), with fitted lognormal distributions. The other observations published by these authors yield very similar approximations to lognormality. Figure 5 shows Faller and Woodcock's (1964) histogram redrawn and with a log-normal curve fitted. The fits are generally as good as one may expect for their respective sample sizes, with the possible exception of Figure 5.

Kenney (1977) also pointed out that the length of individual windrows, although much greater than windrow spacing, is finite, and again a random variable with a

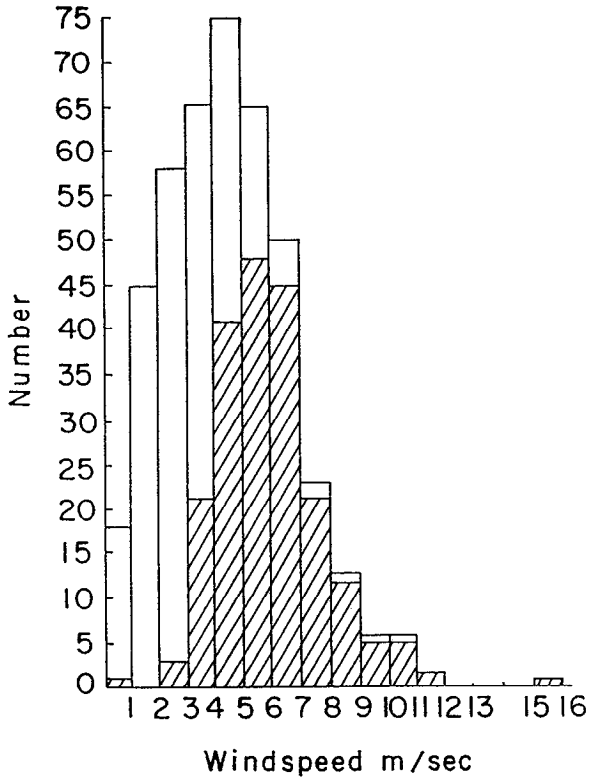

Figure 1. Histogram of windrow occurrence, versus wind speed. Hatched parts of the bars show the number of observations with windrows present, unhatched, windrows absent. From Scott *et al.* (1969).

lognormal distribution. Stommel's (1951) example of "venous" streaks, recently reprinted in a paper of Faller and Auer (1988), vividly illustrates the finite and irregularly varying length of windrows. Thorpe (1992) shows converging as well as finite-length windrows in plan.

How does the lognormal distribution of windrow spacing arise? Aitchison and Brown (1966) show that a process subject to the "law of proportionate effect" produces such a result. That law is, quoting from Aitchison and Brown:

"A variate subject to a process of change is said to obey the law of proportionate effect if the change in the variate at any step of the process is a random proportion of the previous value of the variate."

Kolmogoroff (1941) developed his theory of breakage (of particles of coal, say, in a crushing operation) invoking the same law. Applied to windrow spacing, if a new windrow is generated at a random location (or even a single vortex of a vortex pair), it "breaks up" the preexisting spacing in a random proportion. Windrow generation at

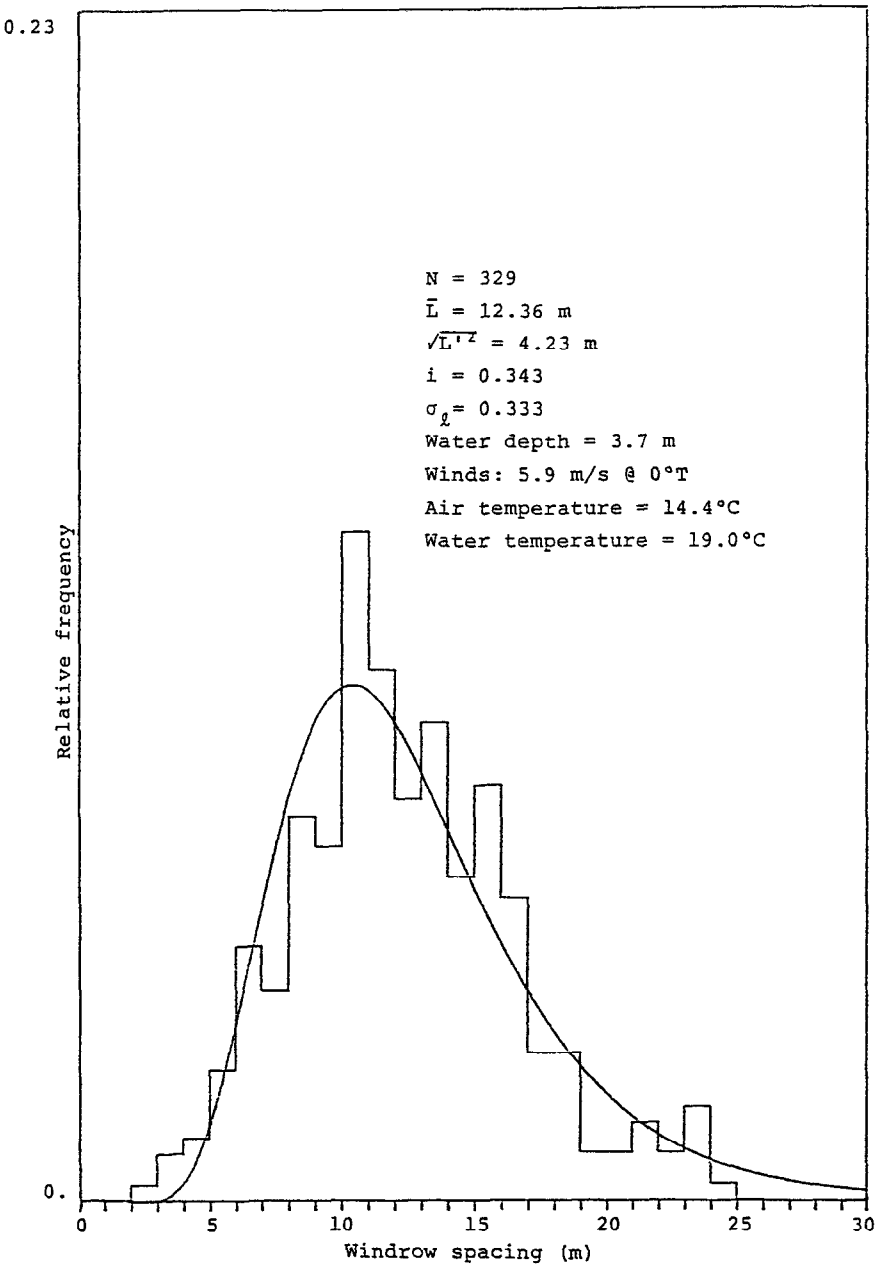

Figure 2. Frequency (fraction of total) of windrow spacing, and fitted log-normal curve. Data of Kenney (1977), taken on the Lake of the Woods.

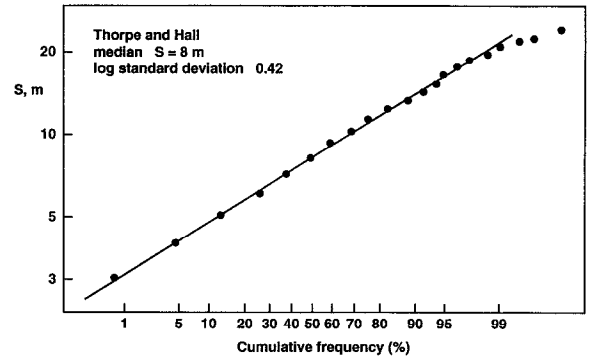

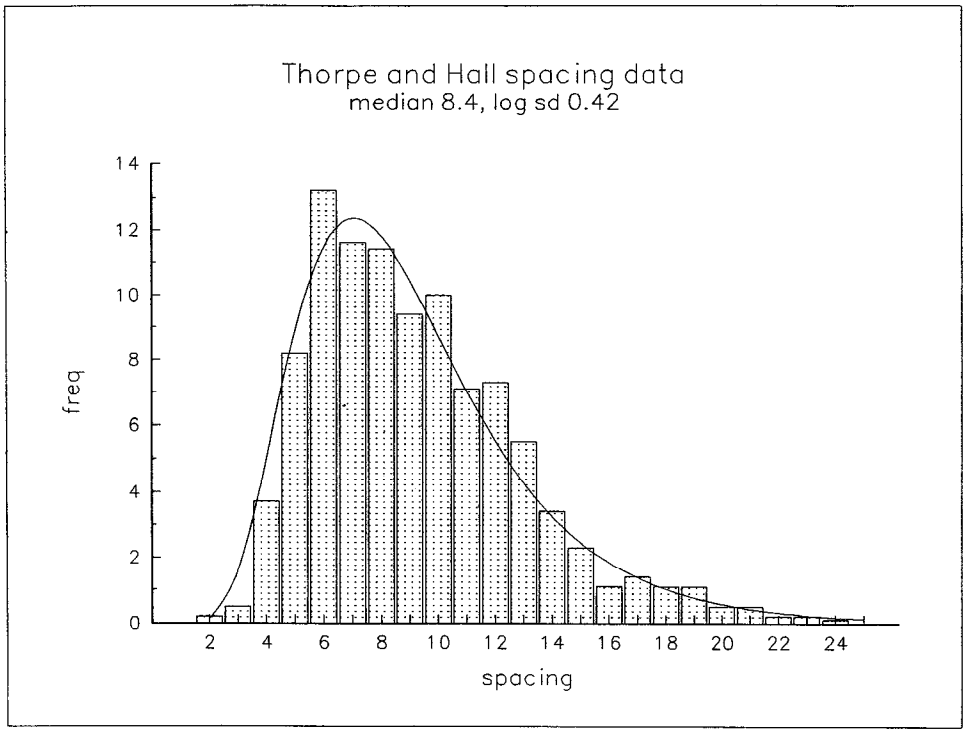

Figure 3. Windrow spacing data of Thorpe and Hall (1982): (a) Cumulative frequency versus logarithm of spacing, on probability paper; (b) Histogram of frequency versus spacing. Dots: data, Line: fitted lognormal distribution.

random locations is thus consistent with the observed lognormal distribution of spacing.

As a further illustration of the highly variable character of windrows, consider some observations from our studies on Lake Huron (Csanady and Pade, 1969). We released floating objects from a line source of uniform strength (arranged across

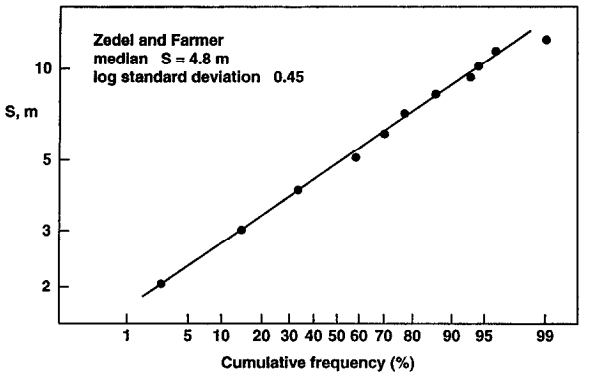

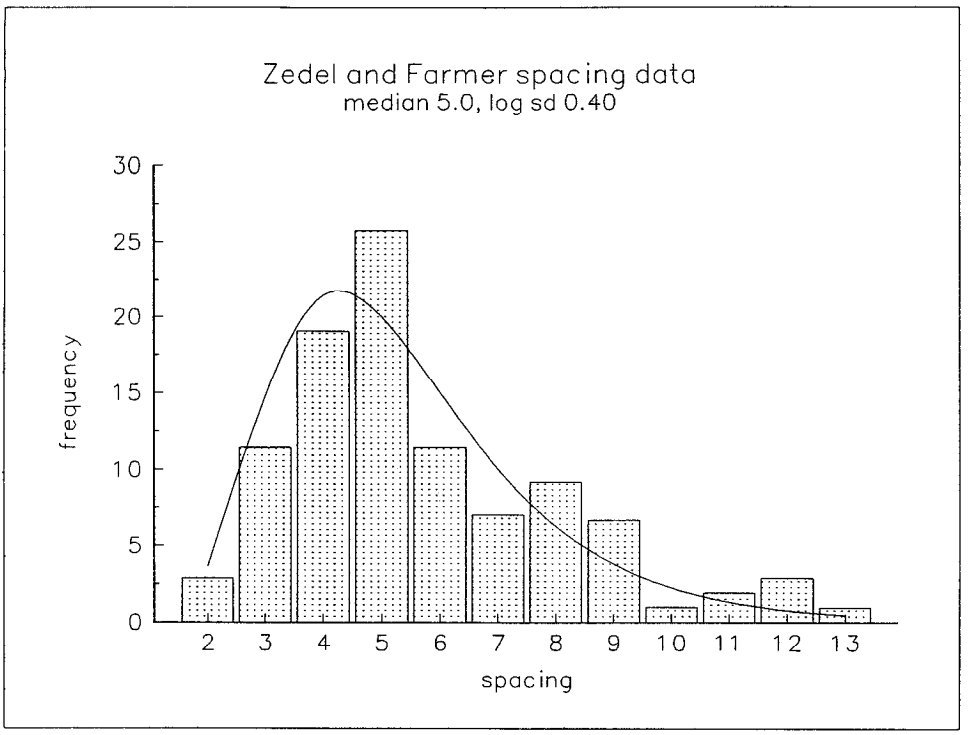

Figure 4. As Figure 3, but data of Zedel and Farmer (1991).

windrows) and caught them in a net downstream. Drift bottles equipped with hooks served as floating objects; a 200 m long net stretched across the current, 200 m downstream of the source, collected them. Of 200 bottles released, we usually collected about half, even when misguessing the surface current direction. We recorded the number of bottles collected at each 2 m length of the net. Figure 6 shows observed bottle distributions along the net, observed on three different occasions. Dominant peaks occur at 10–70 m spacing, with lesser peaks in between.

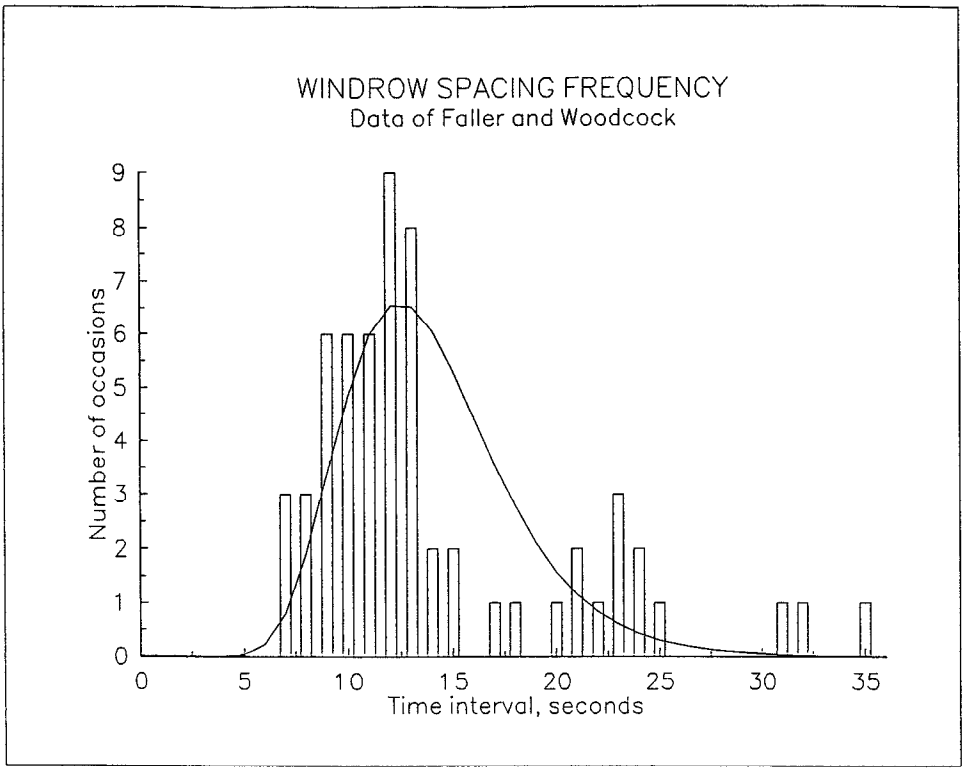

Figure 5. Time elapsed between windrow encounters by a ship crossing them, and fitted log-normal distribution. Histogram redrawn from Faller and Woodcock (1964).

The tall and short bars, indicating numbers caught, presumably signify more or less vigorous convergences.

An important observation is that windrows decay in time, and release their floating markers to other windrows (Csanady, 1974). Our observations, using aluminium powder, confetti, and computer cards suggested windrow lifetimes of order 1000 s. Zedel and Farmer (1991) report that individual bands of bubbles (their windrow markers) retain their identity from 5 to 20 minutes, a very similar estimate. According to Thorpe (1992), windrows persist for 15–30 minutes, again agreeing with other work.

Another remarkable finding is that, upon a change of wind direction, new windrows appear within a few minutes, parallel to the new wind, even though the water 1 m or so below the surface still moves in the old direction. Several investigators reported a similar scenario, beginning with Welander (1963). The rapid response to wind demonstrates that windrows are continually being generated, and that their vortices are at least initially very close to the surface. In view of the emerging picture of a "life-cycle" of windrows, it is reasonable to interpret observa-

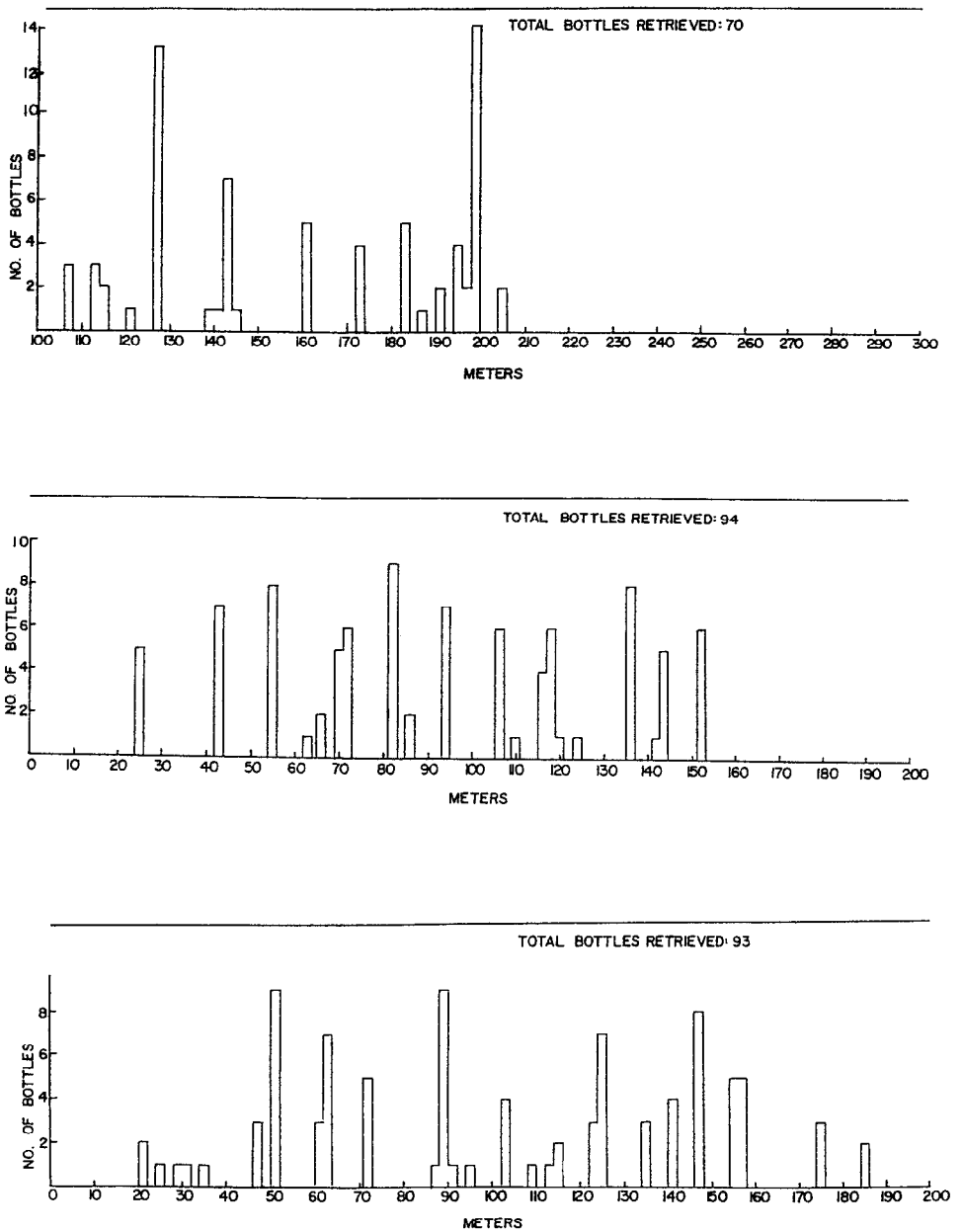

Figure 6. Drift bottles collected 200 m from a line source, per 2 m bin in a net stretched across the wind-driven current. Observations in Lake Huron in the summer of 1969, from a report of limited circulation (Csanady and Pade, 1969).

tions of less vigorous windrows as showing relatively young or old ones, while the dominant ones may be at the peak of their life-cycle.

Summing up the evidence on windrow variability, windrow spacing, length and intensity are random variables, individual windrows go through a cycle of generation and decay. The lognormal distribution of spacing suggests windrow generation at random locations on the sea surface.

3. Generation of streamwise vorticity

The accepted conceptual model of helical particle motions in Langmuir circulation is a superposition of streamwise (windward) shear flow and streamwise vortices (axes parallel to the wind). The principal theoretical difficulty is to account for the origin of the streamwise vortices.

Vortex generation and decay is subject to Helmholtz's theorems, see Lamb (1957, p. 205). Laying the positive x-axis downwind, y crosswind to the left, z vertical, the tendency equation for the material derivative of ξ, the x-component of vorticity, is:

$$\frac{D\xi}{Dt} = \xi\frac{\partial u}{\partial x} + \eta\frac{\partial u}{\partial y} + \zeta\frac{\partial u}{\partial z} + \nu\nabla^2\xi \tag{1}$$

where:

$$\xi = \frac{\partial w}{\partial y} - \frac{\partial v}{\partial z} \qquad \eta = \frac{\partial u}{\partial z} - \frac{\partial w}{\partial x} \qquad \zeta = \frac{\partial v}{\partial x} - \frac{\partial u}{\partial y}$$

The last term in Eq. (1) represents the curl of viscous stresses, the other three terms on the right in order, stretching preexisting streamwise vorticity, and tilting of crosswind and vertical vortex lines. Intuitive ideas on vortex tilting can be misleading: if the streamwise velocity varies spanwise ($\partial u/\partial y$ nonzero), one might think that it tilts the y-component of the vorticity (which is dominated by the $\partial u/\partial z$ term) to produce ξ. In fact, however, the tilting of ζ by $\partial u/\partial z$ exactly cancels this, if x-gradients of u or v are absent. Substituting the definitions of η and ζ into the ξ-equation one finds indeed:

$$\frac{D\xi}{Dt} = \xi\frac{\partial u}{\partial x} + \frac{\partial v}{\partial x}\frac{\partial u}{\partial z} - \frac{\partial w}{\partial x}\frac{\partial u}{\partial y} + \nu\nabla^2\xi \tag{2}$$

which shows that, apart from stretching pre-existing streamwise vorticity, ξ can be generated by vortex tilting only in shear flow with *streamwise* variation of one of the *cross-stream* velocity components, v or w.

Wind-driven shear flow has to coexist with a wind-wave field. A key contribution of Craik and Leibovich (1976) was to show that the wave motion interacts with the shear flow through Stokes drift. By hypothesis, Stokes drift is a residue of irrotational wave motion, and therefore does not contribute to vorticity. Supposing Stokes drift to be

directed downwind, and of magnitude U, the combined streamwise velocity of shear flow and Stokes drift is $U + u$, while vorticity and the other velocity components are of the shear flow alone. If the velocity field does not vary in the x-direction, the tendency equation for ξ becomes Eq. 15 of Craik and Leibovich (1976):

$$\frac{D\xi}{Dt} = \frac{\partial u}{\partial z}\frac{\partial U}{\partial y} - \frac{\partial u}{\partial y}\frac{\partial U}{\partial z} + \nu\nabla^2\xi. \tag{3}$$

In other words, because Stokes drift does not contribute to η or ζ, the cancellation of tilting terms does not take place, and ξ may be generated by Stokes drift varying spanwise (CL1 theory), or by spanwise uniform Stokes drift acting on pre-existing vertical vorticity ζ (CL2 theory).

In the absence of x-gradients, the flow in cross-wind planes may be described by a streamfunction $\phi(y, z)$, such that $\xi = -\nabla^2\phi$. Using this approach, Leibovich and his collaborators have explored the consequences of the CL2 theory in a number of recent contributions, see e.g. Cox and Leibovich (1993), and references given there to earlier work. In these applications of the CL2 theory, a feedback mechanism generates streamwise vorticity: an initially weak spanwise variation of streamwise velocity u, acted upon by Stokes drift, generates streamwise vorticity, which then enhances u-variation. Apart from the initial small perturbation, the shear flow is supposed uniform in the xy plane. While the velocity field averaged over a long enough time undoubtedly approximates this state closely, on shorter time scales the flow is highly variable. Energetic wind gusts produce locally intensified shear flow, of limited extension both along and across wind. On a smaller spatial scale, the "roller" of a breaking long wave exerts shear stresses many times greater than typical wind stress (Duncan 1981; 1983; Battjes and Sakai, 1986; Csanady, 1990a), over a limited area, for a few seconds. In similar events, one cannot rule out without further investigation shear flow-vortex interactions as generators of significant streamwise vorticity. More important, Stokes drift has relatively large, and irregularly distributed, preexisting vorticity to work with, instead of the "initially weak spanwise-periodic circulations" envisaged by Craik (1977) in his initial discussion of the instability mechanism, later to become the CL2 theory.

4. Moving shear stress anomaly model

Wind gusts or breaking waves have in common not only limited horizontal extension, but also rapid alongwind progress. We model their effects by a "moving shear stress anomaly," a horizontal distribution of excess shear stress, translating much faster than the perturbation motions it generates in the water:

$$\tau/\rho = u^{*2}\,\varphi(x - Vt, y) \tag{4}$$

where $\varphi(x, y)$ vanishes at large x and y, u^{*2} is the maximum excess stress, and $V \gg u^*$. When such a stress pattern passes over the water surface, it generates a system of

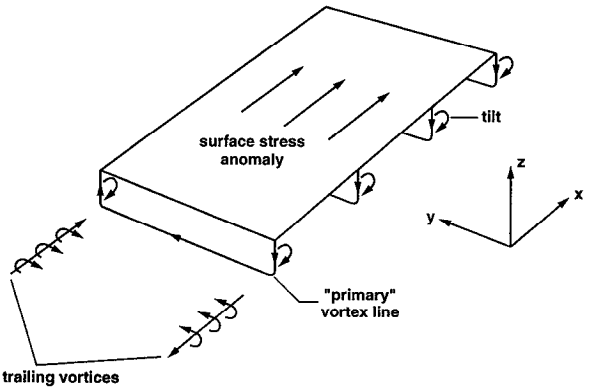

Figure 7. "Primary" vortex lines generated by a surface stress anomaly of limited extent, and trailing streamwise vortices, in a schematic illustration.

"primary" vortex lines in (xz) planes, consisting of crosswind (η) vorticity under the stress anomaly, vertical vorticity (ζ) at the sides, where the vortex lines bend up and terminate at the free surface, see the schematic illustration, Figure 7. The effect of the surface shear stress penetrates only to a small depth, so that the crosswind vortices are all close to the surface, their upturned ends short. The illustration is a snapshot at a fixed time t, because the whole pattern moves rapidly in the wind direction. The fast moving stress anomaly leaves a long wake behind: our object here is to investigate whether streamwise vortices are part of the wake, and if so, what their sign and strength is.

To model the primary flow pattern under the stress anomaly, we represent momentum transfer via breaking wavelets and other surface turbulence by a constant eddy viscosity ν. The limited observational evidence on the velocity distribution immediately below a wind-blown water surface shows that ν is here much smaller than in the body of the mixed layer (Churchill and Csanady, 1983), being in moderate winds of order 1 $cm^2\ s^{-1}$. Free surface shear layer models show surface velocities to be of order $10u^*$, small compared to the translation velocity of the stress anomaly. Linearized equations of motion are then adequate for the calculation of primary velocities, and the solution may be resolved into an irrotational and a viscous part, following the classical approach outlined by Lamb (1957). Well away from the spanwise edges of the stress anomaly the flow pattern should be much as under shear stress anomaly occupying a strip infinite in the spanwise direction. Figure 8 illustrates the flow pattern in an xz plane for this case: a viscous boundary layer grows under the stress anomaly.

The momentum balance of the fluid affected by the stress anomaly involves a pressure gradient $\partial p/\partial x$ arising in response to the forcing. If this were significant, some of the momentum input by the wind would appear as trailing wave momentum. As in problems of wave generation by an obstacle submerged in a stream (Duncan,

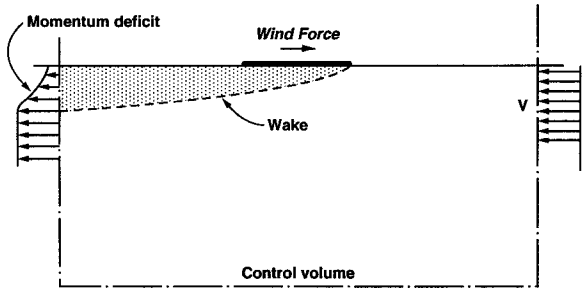

Figure 8. Flow field generated by a moving stress anomaly in the center xz plane, showing wake, and control volume used in momentum balance.

1981), the balance of momentum for the control volume indicated in Figure 8 is: momentum input by the wind equals trailing wave momentum plus wake momentum deficit. Calculation of the split between the two potential momentum sinks, for the case of surface stress forcing, shows 99% plus going into wake momentum deficit (Csanady, 1991). The combined viscous and irrotational solution shows vertical motion under the stress anomaly, due to the displacement effect of the growing viscous boundary layer. The maximum vertical velocity equals u^{*2}/V under the strip, vanishes forward or behind. One may at once conclude that such small velocities (typically of order 10^{-3} cm s^{-1}) cannot generate significant streamwise vorticity.

A simple extension of the infinite strip model to finite width shows spanwise motion generated by the displacement effect of the *lateral* boundary layer along the spanwise edges of the stress anomaly. The analytical solution for this case is the analog of the temperature field of a rectangular surface heat source on a semi-infinite body of moving fluid, see Carslaw and Jaeger (1959, p. 270). It is not difficult to show that the total displacement effect, in the vertical and the lateral directions, is the same as under an infinite strip cut to the length of the finite strip, so that any lateral displacement comes at the expense of vertical velocities. Also, spanwise and vertical velocities are of the same order if the horizontal and vertical viscosities are. Even for very different viscosities, spanwise velocities are still very small. Therefore streamwise vortex generation by the shear flow alone, according to Eq. 2, remains insignificant.

5. Trailing vorticity and circulation

We now turn to the calculation of trailing vorticity. In a coordinate system moving with the stress anomaly the flow is steady, the velocity is $-V$ plus the velocities induced by surface stress forcing. We neglect shear flow vortex interactions, viscous decay, suppose the vertical derivative of the Stokes drift dU/dz to be constant, the total derivative of ξ to be dominated by $V\partial\xi/\partial x$. The tendency equation for ξ then

simplifies to:

$$-V\frac{\partial \xi}{\partial x} = \xi\frac{\partial u}{\partial x} - \frac{dU}{dz}\frac{\partial u}{\partial y}. \tag{5}$$

As the fluid passes under the stress anomaly (now imagined fixed) the streamwise vorticity changes according to this first order differential equation for ξ. Let the stress anomaly extend from $x = -b$ to b. At the trailing edge of the anomaly the streamwise vorticity is then:

$$\xi = -\frac{1}{V}\frac{dU}{dz}\int_{-b}^{b}\frac{\partial u}{\partial y}\exp\left(\frac{u[x'] - u[x]}{V}\right)dx'. \tag{6}$$

Because the primary flow velocities $u(x)$ are small compared to V, the exponential term may be dropped, being nearly unity everywhere. As is intuitively clear from Figure 7, negative vorticity is generated on the right of the anomaly, positive on the left. Of main interest from the point of view of Langmuir circulation is the total vorticity generated over the right-hand and left-hand halves of the anomaly separately, in other words the circulation:

$$\Gamma = \int\int \xi\, dy\, dz \tag{7}$$

with the integration limits from zero to plus and minus infinity along y, minus infinity to zero along z. Substituting Eq. (6) and carrying out the integrations with respect to y leads to, over the right-hand side of the anomaly:

$$\Gamma = -\frac{1}{V}\frac{dU}{dz}\int_{-b}^{b}\int_{-\infty}^{0} u(y = 0)\, dx\, dz. \tag{8}$$

The vertical integral of the velocity u in the center plane $y = 0$ is the momentum deficit discussed in the previous section. If lateral boundary layers do not affect the velocities in the center plane, momentum deficit equals upstream momentum input by the stress anomaly. For constant u^*, the momentum deficit under the stress anomaly increases linearly with distance from the leading edge. The circulation at the trailing edge, and behind, is then:

$$\Gamma = -\frac{1}{2}\frac{dU}{dz}u^{*2}t^2 \tag{9}$$

where we have written $t = 2b/V$ for the duration of the stress anomaly, as perceived at a fixed location. The negative sign applies on the right-hand side of the anomaly, and is to be replaced by the positive sign on the left. The result is remarkable for its simplicity: the strength of the trailing vortices, as measured by their circulation, is independent of viscosity, of the dimensions or speed of the anomaly, except through its local duration. Apart from duration, vortex strength at

the trailing edge of the anomaly is proportional to Stokes drift gradient, and the intensity of the stress anomaly. One may also think of $u^{*2}t$ as the impulse of the stress anomaly, and regard vortex strength as impulse times duration, times Stokes drift gradient. The result applies to stress anomalies of sufficient spanwise width not to smear out the momentum deficit laterally.

The simplicity of Eq. (9) allows quick estimation of left-behind streamwise vortex strength. Taking a modest Stokes drift gradient of 0.1 s^{-1}, a stress anomaly equal to the mean wind stress under moderate wind, (see the gust factors of Smith and Chandler, 1987) 1 cm^2 s^{-2}, and a typical gust duration of 100 s, one arrives at $\Gamma = 500$ cm^2 s^{-1}, at the trailing edge of the anomaly, and behind. A moderately large breaking long wave exerts stresses some hundred times greater (Battjes and Sakai, 1981), but lasts only one tenth as long, and should leave behind vortices of a similar strength.

6. Vortex kinematics near a free surface

The vortex pair left behind by a stress anomaly is analogous to the tip vortices of aircraft (except for a difference in sign: near a free surface the tip vortices would induce divergence rather than convergence between the vortex centers). Theory and observation show that such vortex pairs move relative to the fluid around them. They may also be unstable (Thorpe, 1992), and interact in unexpected ways in turbulent flow, see e.g. Maxworthy (1977). Therefore one must view with caution conclusions based on inviscid fluid mechanics. Nevertheless, it is of interest to explore the inviscid kinematics of a vortex pair near the free surface, as a zero order theory of their interaction.

Suppose therefore that a pair of counterrotating vortices are present, their centers a short distance below the surface (say 1 m or so), separated horizontally by a distance an order of magnitude larger. For simplicity we model the distributed vorticity trailing a stress anomaly by two line vortices below the free surface, in a semi-infinite inviscid fluid at rest. Adding a pair of mirror-image vortices satisfies the boundary condition of zero vertical velocity at the free surface. All four vortices are of the same strength, two of positive (clockwise) sense, two negative, Figure 9. Lamb (1957, p. 223) described the behavior of this vortex system. Initially much farther apart than their depth by hypothesis, the vortices move closer together, under the influence of the image vortices. As they approach each other, they induce strong convergence and downwelling near their plane of symmetry. Finally they dive down and move vertically away from the surface, but remain close together. The equation of vortex path, $Y(Z)$, is, with the origin of the yz coordinates at the surface, in the plane of symmetry:

$$Y^2Z^2 = b^2(Y^2 + Z^2) \tag{10}$$

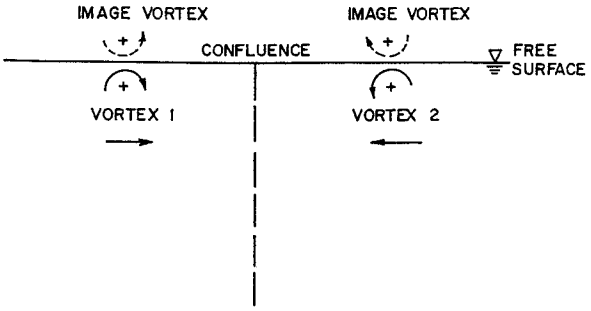

Figure 9. Vortex pair left behind by a surface stress anomaly moving with the wind. The image vortices induce converging motion of the vortex pair.

where $2b$ is the asymptotic separation of the vortices at large Y or Z. The paths of the two vortices are mirror images.

A vortex at (Y, Z) has a horizontal velocity given by (Lamb, 1957):

$$\frac{dY}{dt} = -\frac{\Gamma}{4\pi}\frac{Y^2}{Z(Y^2 + Z^2)}. \tag{11}$$

From this formula it is a simple matter to calculate the time elapsed between vortex positions (Y_o, Z_o) and (Y, Z):

$$t = \frac{\pi b^2}{\Gamma}(Y_o/Z_o - Y/Z - Z_o/Y_o + Z/Y). \tag{12}$$

Supposing the initial separation of the vortices to be about ten times their depth, the time taken to sink five times deeper than their initial depth is about $t = 9.6\pi b^2/\Gamma$. This is an order of magnitude "lifetime" estimate. Note that the lifetime is inversely proportional to vortex strength.

The flow field induced by the vortices is two-dimensional in the yz plane, described by a streamfunction $\psi(y, z)$, such that $w = \partial\psi/\partial y$, $v = -\partial\psi/\partial z$. The equation of the streamlines, accounting for both the "real" and the image vortices, is:

$$\psi = \pm\frac{\Gamma}{2\pi}[\ln(r_1 r_4) - \ln(r_2 r_3)] \tag{13}$$

where Γ is the strength (circulation) of each vortex, and $r_i = [(y - Y_i)^2 + (z - Z_i)^2]^{1/2}$, $i = 1 - 4$, is the radius drawn from each vortex, (Y_i, Z_i) to a point (y, z). Velocities may be calculated from this equation. The intersection of the vortex systems' two planes of symmetry, $(y = 0, z = 0)$ is a stagnation- and convergence-line

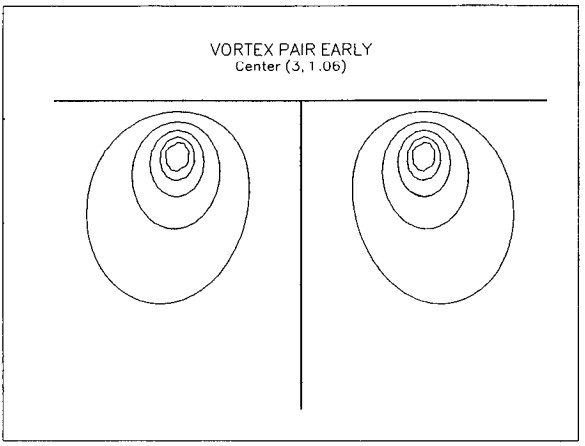

Figure 10. Streamlines of flow induced by a vortex pair, when the vortices are still some distance from the convergence line.

of the flow. At the time of closest approach of the vortices to the convergence line ($\pm Y$, $-Z = \sqrt{2}\,b$) the horizontal surface velocity is distributed as:

$$v = -\frac{\Gamma}{\pi b}\frac{y}{(y/2)^4 + 1}. \tag{14}$$

The maximum convergence velocity is then $v = 1.14\ \Gamma/b\pi$: this is also the maximum downwelling velocity w, reached at the same time as the maximum convergence velocity, when the $v(y, 0)$ and $w(0, z)$ distributions are identical.

While the vortices are still relatively far apart, the main feature of their flow field is surface motion directed toward the plane of symmetry, and only weak convergence, see streamlines in Figure 10. At their closest approach to the convergence line (the "peak of their life cycle, Fig. 11) the vortices induce strong convergence and downwelling. Later, when the vortices have moved to relatively large depth, Figure 12, the flow picture is again as in Figure 10, but with the roles of the y and z axes reversed: there is strong downward motion at depth, and not much surface motion or convergence.

The emerging picture is of an essentially unsteady phenomenon, in place of the steady-state, closed streamline, roll-circulation envisaged in earlier theories of Langmuir circulation. Putting together the arguments of the previous section with the results here, we have arrived at the conceptual model of a stress anomaly moving with the wind (or with a breaking long wave) and leaving counterrotating vortices in its wake, which converge and disappear at depth, even as an inviscid flow phenomenon, without taking into account inevitable decay.

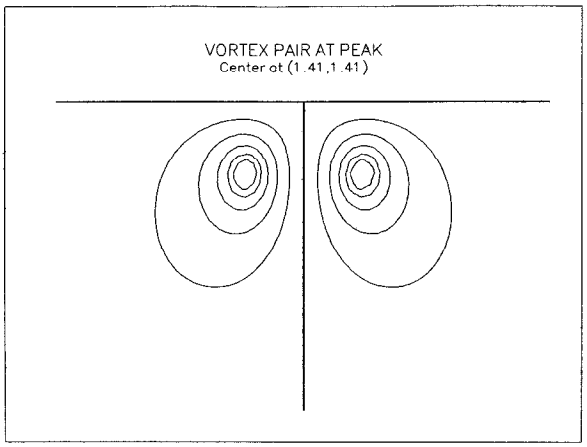

Figure 11. Streamlines of induced flow at the time of closest approach to the convergence line.

7. Windward surface velocity

It remains to account for the increase of the streamwise (windward) component of surface velocity in Langmuir circulation. In general terms, the explanation is clear from first principles: while the fluid is moving from upwelling to downwelling regions, wind-imparted momentum increases its streamwise velocity. Without further investigation it is not clear, however, that the resulting increase in surface velocity is significant.

Consider the shear flow now (away from stress anomalies), together with a pair of very long Langmuir vortices (so that there is no significant streamwise pressure- or velocity-gradient). Constant wind stress action on the surface and Langmuir circulation combine to create perturbations on the mean streamwise velocity distribution, $u'(y, z)$, the strength of which we want to estimate. Given the short lifetime of Langmuir vortices, we can safely neglect the Coriolis force. At the same time, we can suppose the lifetime long enough to neglect the local time derivative of streamwise velocity in comparison with advective change (due to Langmuir circulation), except near the convergence line where v and w vanish. With surface eddy viscosity small, we expect a thin surface boundary layer to form, allowing neglect of cross-stream diffusion of streamwise momentum in comparison with advection. Streamwise momentum balance and continuity of the perturbing motions are then:

$$v\frac{\partial u'}{\partial y} + w\frac{\partial u'}{\partial z} = \nu\frac{\partial^2 u'}{\partial z^2}$$

$$\frac{\partial v}{\partial y} + \frac{\partial w}{\partial z} = 0. \tag{15}$$

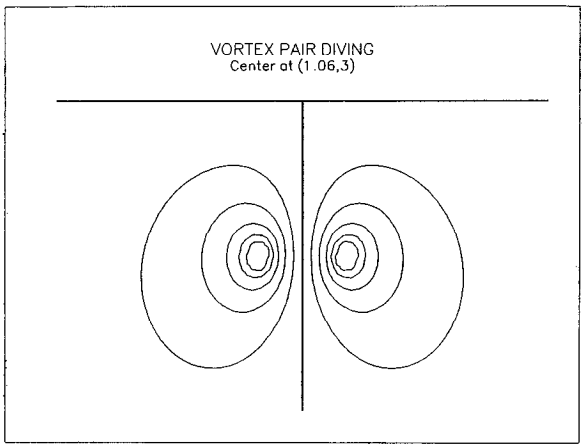

Figure 12. Streamlines after the vortex pair has moved well downward.

The boundary condition at the surface is:

$$u^{*2} = \nu \frac{\partial u'}{\partial z}$$

where ρu^{*2} is wind stress. The problem posed by these equations is the same as advection-diffusion of a scalar property (for example gas concentration, Csanady, 1990b) in a surface diffusion boundary layer, over a large eddy. In the present case, windward momentum (constant density times the velocity perturbation u') is the diffusing quantity, the flux of which is prescribed at the surface. Neglect of Coriolis force and windward pressure gradient of course oversimplifies the problem: over the depth of the mixed layer the wind stress is either balanced by one of these, or else the mixed layer accelerates. Eqs. 15 describe dominant balances in a thin surface layer, where the shear stress gradient is balanced by slow-fluid advection. The implied bulk balance is that the Langmuir circulation advects the momentum acquired at the surface into the body of the mixed layer. This situation prevails if the Peclet number vl/ν of the Langmuir circulation (v = typical velocity, l scale, ν eddy viscosity near the surface) is much larger than unity, a condition usually well satisfied.

An analytical solution of Eqs. 15, satisfying the surface boundary condition is (Csanady 1990b):

$$u' = (u^{*2}/v\nu)\sqrt{2\nu q}\, ierfc(\psi/\sqrt{2\nu q}) \tag{16}$$

where ψ is streamfunction of the Langmuir circulation in the yz plane, v is crosswind surface velocity, $q = \int v\, dy$ its line integral. The boundary layer solution breaks down near the convergence line where v vanishes. Away from that singularity, putting realistic numbers into Eq. (19), $u^* = 1$ cm s^{-1}, $\nu = 1$ cm^2 s^{-1}, $v = 3$ cm s^{-1}, $q = 1000$ cm^2 s^{-1} (v times a cross-stream travel distance of about 3 m), one finds for the

surface velocity u' $(q, 0) = 2.5$ cm s^{-1}, at a boundary layer thickness of $\sqrt{2\nu q}/\nu =$ 15 cm. The boundary layer is thin enough to suppose ν = constant, the Reynolds number based on boundary layer thickness large enough to justify the boundary layer approximation. The surface velocity increment in 3 m cross-stream travel (or in about 100 s exposure) is 15% or so of typical surface velocities in moderate winds, a significant increase. At the convergence line horizontal mixing must sustain a finite excess velocity, which should be an even higher percentage of the mean surface velocity.

8. Discussion

How realistic is this limited-lifetime vortex pair model of Langmuir circulation? Observations of Langmuir and others have suggested a downwelling velocity of order 3 cm s^{-1}. A realistic guess at the effective vortex depth is $b = 1$ m: this gives, from Eq. 14, Γ of order 1000 cm^2 s^{-1}, in good agreement with the estimates of vortex strength left behind a moving shear stress anomaly using Eq. 9. The corresponding "lifetime" estimate from Eq. 12, defined above as the time it takes for the vortices to move from their initial fairly large separation to a depth five times their initial depth, is 300 s. Observation suggested lifetimes of order 1000 s, meaning the time for an established windrow to dissolve. Given the different definitions of lifetime, the estimates are reasonably close.

Another well established feature of Langmuir circulation is that downwelling speeds are higher than upwelling ones. This is certainly the case in the vortex pair model, while the vortices are close to their convergence line, i.e. over most of their "lifetime," as Figures 10 to 12 illustrate. The last of these, showing a vortex pair at depth, may portray a situation similar to that reported by Weller and Price (1988), with large sinking velocity in the middle of the mixed layer.

The principal merit of the moving stress anomaly model is, however, that it accounts for the stochastic nature of windrows, and allows room for the great variability of their observed properties. Apparently conflicting evidence on downwelling speed, or even on the presence or absence in winds of similar strength, can be understood if random external forcing is the primary cause of Langmuir circulation. If gustiness of wind, or wave breaking, are important prerequisites of windrow formation, their occurrence or properties depend on more than just wind speed.

Acknowledgments. This work has been supported by the Dept. of Interior, Minerals Management Service.

REFERENCES

Aitchison, J. and J. A. C. Brown. 1966. The Lognormal Distribution. Cambridge Univ. Press, 176 pp.

Battjes, J. A. and T. Sakai. 1981. Velocity field in a steady breaker. J. Fluid Mech., *111,* 421–437.

Carslaw, H. S. and J. C. Jaeger. 1959. Conduction of Heat in Solids, second ed. Oxford Univ. Press, London, 510 pp.

Churchill, J. H. and G. T. Csanady. 1983. Near-surface measurements of quasi-Lagrangian velocities in open water. J. Phys. Oceanogr., *13,* 1669–1680.

Cox, S. M. and S. Leibovich. 1993. Langmuir circulations in a surface layer bounded by a strong thermocline. J. Phys. Oceanogr., *23,* 1330–1345.

Craik, A. D. D. 1977. The generation of Langmuir circulations by an instability mechanism. J. Fluid Mech., *81,* 209–223.

Craik, A. D. D. and S. Leibovich. 1976. A rational model for Langmuir circulations. J. Fluid Mech., *81,* 209–223.

Csanady, G. T. 1965. Windrow studies. Great Lakes Inst. Univ. Toronto report No. PR 26, 60–82.

—— 1974. Turbulent diffusion and beach deposition of floating pollutants. Adv. Geophys. Suppl., *18A,* 371–381.

—— 1990a. Momentum flux in breaking wavelets. J. Geophys. Res., *95,* 13,289–13,299.

—— 1990b. The role of breaking wavelets in air-sea gas transfer. J. Geophys. Res., *95,* 749–759.

—— 1991. Wavelets and air-sea transfer. Air-water mass transfer, Second International Symposium, 563–581, published by ASCE.

Csanady, G. T. and B. Pade. 1969. Windrow observations. Dynamics and diffusion in the Great Lakes, Univ. Waterloo Dept. Mech. Engr. report, 3–38.

Duncan, J. H. 1981. An experimental investigation of breaking waves produced by a towed hydrofoil. Proc. Roy. Soc. London, *A377,* 331–348.

—— 1983. The breaking and non-breaking resistance of a two-dimensional aerofoil. J. Fluid Mech., *126,* 507–520.

Faller, A. J. 1971. Oceanic turbulence and the Langmuir circulations. Ann. Rev. Ecol. Syst. *2,* 201–236.

Faller, A. J. and S. J. Auer. 1988. The roles of Langmuir circulations in the dispersion of surface tracers. J. Phys. Oceanogr., *18,* 1108–1123.

Faller, A. J. and A. H. Woodcock. 1964. The spacing of windrows of Sargassum in the ocean. J. Mar. Res., *22,* 22–29.

Gargett, A. E. 1989. Ocean turbulence. Ann. Rev. Fluid Mech., *21,* 419–451.

Kenney, B. C. 1977. An experimental investigation of the fluctuating current responsible for the generation of windrows. Ph.D. thesis, University of Waterloo, 163 pp.

Kolmogoroff, A. N. 1941. Über das logarithmisch normale Verteilungsgesetz der Dimensionen der Teilchen bei Zerstückelung. C. R. Acad. Sci. U.R.S.S. *31,* 99.

Lamb, H. 1957. Hydrodynamics. Cambridge Univ. Press, 738 pp.

Langmuir, I. 1938. Surface motion of water induced by wind. Science, *87,* 119–123.

Leibovich, S. 1983. The form and dynamics of Langmuir circulations. Ann. Rev. Fluid. Mech., *15,* 391–427.

Leibovich, S. and S. Paolucci. 1980. The Langmuir circulation instability as a mixing mechanism in the upper ocean. J. Phys. Oceanogr., *10,* 186–207.

Leibovich, S. and A. Tandon. 1993. Three-dimensional Langmuir circulation instability in a stratified layer. J. Geophys. Res., *98,* 16,501–16,507.

Maxworthy, T. 1977. Some experimental studies of vortex rings. J. Fluid Mech., *81,* 465–495.

Pollard, R. T. 1977. Observations and theories of Langmuir circulations and their role in near-surface mixing. Voyage of discovery, George Deacon 70th anniversary volume, Deep-Sea Res., Supplement, 235–251.

Scott, J. T., G. E. Myer, R. Stewart and E. G. Walther. 1969. On the mechanism of Langmuir circulations and their role in epilimnion mixing. Limnol. Oceanogr., *14,* 493–503.

Smith, J., R. Pinkel and R. A. Weller. 1987. Velocity structure in the mixed layer during MILDEX. J. Phys. Oceanogr., *17,* 425–439.

Smith, S. D. and P. C. P. Chandler. 1987. Spectra and gust factors for gale force winds. Boundary Layer Meteor., *40,* 393–406.

Stommel, H. 1951. Streaks on natural water surfaces. Weather *6,* 72–74.

Thorpe, S. A. 1992. The breakup of Langmuir circulation and the instability of an array of vortices. J. Phys. Oceanogr., *22,* 350–360.

Thorpe, S. A. and A. J. Hall. 1982. Observations of the thermal structure of Langmuir circulation. J. Fluid Mech., *114,* 237–250.

Welander, P. 1963. On the generation of wind streaks on the sea surface by action of surface film. Tellus, *15,* 67–71.

Weller, R. A., J. P. Dean, J. Marra, J. F. Price, E. A. Francis and D. C. Boardman. 1985. Three-dimensional flow in the upper ocean. Science, *227,* 1552–1556.

Weller, R. A. and J. F. Price. 1988. Langmuir circulation within the oceanic mixed layer. Deep-Sea Res., *35,* 711–747.

Woodcock, A. H. 1944. A theory of surface water motion deduced from the wind-induced motion of the Physalia. J. Mar. Res., *5,* 196–205.

Zedel, L. and D. Farmer. 1991. Organized structures in subsurface bubble clouds: Langmuir circulation in the open ocean. J. Geophys. Res., *96,* 8889–8900.

Received: *11 May, 1993;* revised: *21 February, 1994.*